SPE 115723

Production Improvement of Heavy-Oil Recovery by Using Electromagnetic Heating

M.A. Carrizales, Larry W. Lake, and R.T. Johns, SPE, University of Texas at Austin

This paper was prepared for presentation at the 2008 SPE Annual Technical Conference and Exhibition held in Denver, Colorado, USA, 21–24 September 2008.

Abstract

Heavy oil is produced primarily by reducing its viscosity using well-known processes such as steam injection, steamsoak, and in situ combustion. A recent technique for recovery consists of resistively heating the reservoir using electrical energy. Resistive heating can be particularly beneficial for reservoirs in which conventional steam operations are uneconomic.

Resistive heating is a special case of a more general form of heating based on electromagnetic energy (EM). EM has the following advantages over steam injection: it can be used to recover extremely heavy hydrocarbon, is not susceptible to heat losses through a wellbore, and its water requirements are far less than for steam. Compared to resistive heating, EM heats within the formation. Thus (for downhole generation) larger well spacing may be possible.

Although its potential was recognized in the late 70's, there are relatively few field applications of EM heating and even fewer engineering studies. The purpose of this paper is to examine how the performance response of EM compares to resistive heating.

This paper presents a model for single-phase flow to calculate the temperature distribution, and the productivity improvement obtained when an EM heating source (an antenna) is placed in a well. We consider both counter-current flow, in which the well with the antenna is also a producer, and co-current flow where the flow is opposite to EM energy flow. Flow is taking place concurrently with the addition of EM energy.

Steady-state solutions for counter-current flow showed a relative productivity index (PI) increase of 2.5 - 12.0 times cold oil production when the input power was varied from 20 to 150kw. A peak improvement occurred when the adsorption coefficient was between $1e^{-3}$ and $1e^{-1}$ m^{-1}, which indicates that there is an optimum adsorption coefficient. Resistive heating is the special case of an infinite adsorption coefficient and the existence of an optimum suggests that EM heating can be more effective than resistive heating. For co-current flow, the improvement was even greater for the same input power. Calculated energy gains (the ratio of produced to injected energy) were in the 8 to 163 range; successful steam injection processes have gains of around 10.

Introduction

Conventional thermal recovery processes such as steam injection, steam soak, and in situ combustion inject one fluid to change oil properties in situ to make it flow easier. Therefore, there are complications of generating, transporting (while avoiding excessive heat losses), and disposing the injected fluid. Electromagnetic heating (EM) does not require a heat transporting fluid, which can be particularly beneficial for deep reservoirs and thin pay-zones where conventional methods are not cost-effective due to excessive heat loss through the adjacent formations (Chakma and Jha 1992). Furthermore, conventional oil field and electrical equipment can be used, which makes this technique attractive where available space is limited as would be the case on offshore facilities. The components of the equipment required for EM heating has been described elsewhere (Bridges et al. 1985; Haagensen 1986; Sierra et al. 2001) and will not be covered in this paper. Since EM heats instantaneously from within, this method is independent of the low thermal conductivity of the oil sand and is unaffected by permeability variations within the formation (Kim 1987).

Electrical heating applications can be divided into two categories based on the frequency of the electrical current used by the antenna:

(1) Low frequency currents are used in electrical resistive heating (ERH) and are less than 60 Hz so that, resistance heating dominates the process;

(2) High frequency currents are used in microwave heating (MW) or radio frequency (RF) heating. These frequencies may vary from kHz to MHz level, and in this mode dielectric heating dominates the process (Kim 1987; Kumar et al. 2000; Sierra et al. 2001). In this paper, EM heating refers to heating produced by the absorption of EM energy by the molecules in the formation. We consider the entire frequency range of energy.

Several authors have studied the effect of ERH on the oil production response. (Wattenbarger and McDougal 1988; Baylor and Wattenbarger 1990). Hiebert et al. (1986) showed that the use of multiple electrodes per well as well as the use of horizontal wells as electrodes could be effective for heating heavy-oil formations with low frequency electrical heating. However, very few papers have appeared for EM heating. Although its potential was recognized since the late 1970's, there are few field applications of EM heating or comprehensive modeling efforts. Abernethy (1976) derived an expression for the EM power attenuation term, later studied by Fanchi (1990) that allows calculating the temperature profile of a reservoir undergoing EM heating. In his work, Abernethy coupled EM adsorption and fluid flow in a one-dimensional radial model for flow performance. To simplify the equations for the model, he neglected heat conduction and heat losses to adjacent formations. Models that account for more physical effects were developed later, although at increasing complexity (McPherson et al. 1985; Fanchi 1990; McGee and Vermeulen 1996).

Field applications of EM heating are scarce for high frequency heating. Kasevich et al. (1994) conducted a pilot using a borehole radio frequency (RF) antenna to demonstrate the ability of EM heating to heat a confined zone without heating the entire reservoir and thereby raise the near wellbore temperature to increase oil production

This paper presents a model for single-phase flow to calculate the temperature distribution, and the productivity improvement obtained when an EM heating source (an antenna) is placed in a well, thermal convection and conduction were included in the model. We consider both counter-current flow, in which the well with the antenna is also a producer, and co-current flow where the flow is opposite to EM energy flow. **Fig. 1** and **Fig. 2** show a schematic view of the EM process for the cases considered. In all cases we introduce EM energy during fluid flow.

Mathematical Model

The energy balances are done on two phases, a so-called "photon" phase that transport the EM energy, and the conventional "material" phase where the reservoir and the oil phase reside. The analytical equation that describes the heating of an oil reservoir is based on an energy balance that allows heat transfer by convection and conduction, and accounts for the radiated EM power as a heat source. Heat loss through the confining layers is as yet unaccounted for.
In terms of heat fluxes, the energy on the material phase can be written in one dimension as

$$M_T \frac{\partial T}{\partial t} = \frac{1}{A(x)} \frac{d(Ae)}{dx} + \frac{1}{A(x)} \frac{d\left(Aq^r\right)}{dx} \tag{1}$$

The terms e and q^r in Eq. 1 are the material and EM fluxes, respectively. The material flux is given by:

$$e = M_o u_o T - k_T \frac{dT}{dx}$$

where the terms on the right represent convention (reference temperature of zero) and conduction, respectively. Substitution of the heat flux by conduction as well as the EM flux into Eq. 1 gives,

$$M_T \frac{\partial T}{\partial t} = M_o u_o \frac{\partial T}{\partial x} - \frac{1}{A(x)} \frac{\partial}{\partial x}\left(A(x) k_T \frac{\partial T}{\partial x} \right) + \alpha q^r \tag{2}$$

In Eq. 2 the volumetric flow rate (u_o), the total volumetric heat capacity (M_T), the fluid volumetric heat capacity (M_o), and the thermal conductivity (k_T) are constants. The term $A(x)$ is to allow for an arbitrary coordinate system as discussed below, the x is the distance coordinate. The last term on the right side of Eq. 2 is the gain in heat content because of the power applied through the "photon" phase as discussed by Bird et al. (2002). The mathematical expression for this term results from the solution of a steady-state energy balance on the photon phase. The steady-state solution is known as Lambert's law of absorption, widely used in spectrophotometry[17], later used by Abernethy[9] for radial flow. It is derived below. The steady-state one-dimensional energy balance for the photon phase is given by:

$$0 = -\frac{1}{A(x)} \frac{d\left(Aq^r\right)}{dx} - \alpha q^r \tag{3}$$

where A is the cross-sectional area. Eq. 3 applies to any coordinate system (e.g. $A = 2\pi r$ for cylindrical coordinates). Eq. 3 is always at steady-state because the mass of the photons is negligible.

An important quantity in all of our results is the adsorption coefficient, α. This quantity is a strong function of other quantities: wavelength of the EM energy, the fluids content and identity, to name a few. We take it as a constant here.
Integration of Eq. 3 gives the following solution,

$$q^r = \frac{\left(Aq^r\right)_{x=x_0}}{A} e^{-\alpha(x-x_0)} \tag{4}$$

where $q^r\Big|_{x=x_0} = \frac{P_0}{A}$ is the constant EM heat flux at the inner boundary. Eq. 4 can be also applied to any coordinate system by substituting the correspondent *A*, and the difference at any distance to the respective inner boundary. Then, for Cartesian flow,

$\Delta x = x - x_0$, for cylindrical flow

$\Delta r = r - r_w$, and

$\Delta r = r^2 - r_0^2$ for spherical flow.

Steady-State Solutions

We used steady-state solutions as a means of:

(1) Validating the transient behavior (below) and
(2) Estimating the maximum productivity improvement possible.

a) Fluxes.

One of the advantages of EM heating is that energy can be transmitted deep into the reservoir. For steady-state flow in a Cartesian coordinate system, Eq. 1 becomes,

$$0 = \frac{de}{dx} + \frac{dq^r}{dx}$$

so that $e + q^r = C$, and the fluxes are constant.

The material energy flux is always opposite to the photon flux, where

$$e = C - q^r = C - q_0^r e^{-\alpha(x-x_0)}$$

The constant C is determined by the nature of the flow, as shown in **Fig. 3**. If the flow is counter-current, *C=0* (Fig. 3 upper); if it is co-current flow $C = q_0^r$ (Fig. 3 lower). The depth of penetration is entirely governed by α; large values indicating short penetration distances. For resistive heating, $\alpha \to \infty$, and the penetration distance is zero, which means that the energy must be transported entirely through the material phase (that is by conduction). The increased depth of penetration of energy transport is a potential improved efficiency that EM has compared to resistive heating.

b) Temperature.

For Cartesian one-dimensional flow, we solved Eq. 2 analytically for steady state counter-current and co-current flow, with solutions of the form:

$$T = T_0 + \frac{q_o^r}{u_o M_o - \alpha k_T}\left(e^{-\alpha x} - e^{-\alpha L}\right) + \frac{\alpha q_o^r k_T}{\left(u_o M_o - \alpha k_T\right) u_o M_o}\left(e^{\frac{-M_o u_o}{k_T}L} - e^{\frac{-M_o u_o}{k_T}x}\right) \tag{5}$$

for counter-current flow, and

$$T = T_0 + \frac{q_o^r}{u_o M_o + \alpha k_T}\left(1 - e^{-\alpha x}\right) + \frac{\alpha q_o^r k_T}{\left(u_o M_o - \alpha k_T\right) u_o M_o} e^{-\alpha L}\left(e^{\frac{-M_o u_o}{k_T}L} - e^{\frac{M_o u_o}{k_T}(x-L)}\right) \tag{6}$$

for co-current flow. Derivations of Eq. 5 and Eq. 6 are in Appendix A. **Fig. 4** shows the steady-state temperature profiles for both counter and co-current flow for linear one-dimensional flow for different values of the adsorption coefficient, α, using the 140 MHz and 915 MHz frequencies taken from Ovalles (2002).

For one-dimensional radial flow, Eq. 2 was solved, assuming steady state, for counter current flow obtaining the following solution,

$$T^* = \frac{P_0 e^{\alpha r_w}}{2\pi h k_T}\left[\left(\frac{r_e}{r}\right)^{\frac{M_o q_o}{2\pi h k_T}}\left(\alpha r_e\right)^{-\frac{M_o q_o}{2\pi h k_T}}\Gamma\left(\frac{M_o q_o}{2\pi h k_T}, \alpha r_e\right) - \left(\alpha r\right)^{-\frac{M_o q_o}{2\pi h k_T}}\Gamma\left(\frac{M_o q_o}{2\pi h k_T}, \alpha r\right)\right]$$
$$+ \frac{P_0}{M_o q_o}\left(\left(\frac{r_e}{r}\right)^{\frac{M_o q_o}{2\pi h k_T}} - 1\right) + T_0\left(\frac{r_e}{r}\right)^{\frac{M_o q_o}{2\pi h k_T}} + \left(1 - \left(\frac{r_e}{r}\right)^{\frac{M_o q_o}{2\pi h k_T}}\right)T^*\Big|_{r_w} \tag{7}$$

where $T^*\Big|_{r_w}$ is the temperature at the wellbore defined as,

$$T^*\Big|_{r_w} = \frac{\frac{P_0 e^{\alpha r_w}}{2\pi h k_T}\left[\left(\frac{r_e}{r_w}\right)^{\frac{M_o q_o}{2\pi h k_T}}(\alpha r_e)^{-\frac{M_o q_o}{2\pi h k_T}}\Gamma\left(\frac{M_o q_o}{2\pi h k_T}, \alpha r_e\right) - (\alpha r_w)^{-\frac{M_o q_o}{2\pi h k_T}}\Gamma\left(\frac{M_o q_o}{2\pi h k_T}, \alpha r_w\right)\right] + \frac{P_0}{M_o q_o}\left(\left(\frac{r_e}{r}\right)^{\frac{M_o q_o}{2\pi h k_T}} - 1\right) + T_0\left(\frac{r_e}{r_w}\right)^{\frac{M_o q_o}{2\pi h k_T}}}{\left(\frac{r_e}{r_w}\right)^{\frac{M_o q_o}{2\pi h k_T}}} \quad (8)$$

A derivation of Eq. 7 is also in Appendix A. **Fig. 5** shows the steady state solutions obtained for one-dimensional radial flow for counter and co-current flow for the same α as above.

c) Productivity Improvement.

Once the temperature distribution along the medium has been determined, the viscosity variation at any distance from the wellbore can be calculated using any available temperature-viscosity correlation. Here we used a viscosity-temperature relationship of the form:

$$\mu(r) = De^{F/T(r)} \quad (9)$$

where *D* and *F* are empirical constants determined from the viscosity measured at two known temperatures. In this paper, we used a value of $D = 4.934E10^{-5}$ mPa-s, and $F = 5726.22$ K determined from viscosity values of an 11° API crude taken from Kim (1987). Appendix B gives the formulas used to calculate the steady-state productivity increase.

Transient Solutions

Because of extensive complexity, transient solutions must be taken numerically.

a) Temperatures. Constant rate.

Steady-state solutions omit an important factor in thermal oil recovery, namely the thermal mass of the rock and fluids. To include this we must make a transient solution.

Eq. 2 was solved using COMSOL Multiphysics for both Cartesian, and cylindrical coordinates for counter and co-current flow. This software allows solution of one or more partial differential equations (PDEs), by finite elements. For transient flow, results will depend on the boundary condition at the well.

For constant flow rate, the temperature increases with time until it reaches the steady-state solution. **Fig. 6** shows the temperature profile for a heavy oil reservoir (11 °API), with 28% porosity, 9 m thickness, and a drainage radius of 15 m, after 30 days of heating for different flow rates using a source of 63 kW for radial counter-current flow. Initial reservoir temperature was 310.927K (100°F). To validate the solutions obtained from COMSOL, analytical solutions for linear and radial flow were developed for the restrictive case of no conduction using a similar procedure as presented in Araque (2002), and compared to the solutions obtained using COMSOL under the same assumption. We also validated the solutions against the steady-state solutions given above.

b) Temperatures. Constant Pressure at the wellbore.

For a constant pressure difference, Eq. 2 was solved with the continuity equation using COMSOL. For single-phase flow, introducing Darcy's law, the fluid flow conservation equation can be written in general form as,

$$\phi c_t \frac{\partial P}{\partial t} - \frac{1}{A}\frac{\partial}{\partial x}\left(\frac{kA}{\mu_o(T)}\frac{\partial P}{\partial x}\right) = 0 \quad (10)$$

Initially a constant rate for a finite time step is assumed. This rate is constrained by the pressure drop, and the temperature-dependent viscosity. Then, Eq. 2 is solved to get the new temperature distribution so the viscosity profile is updated. Using the new viscosity as an input for Eq. 10, the new flow rate can be calculated. This rate being held constant for the next time step, allows us to calculate a new temperature distribution. This procedure is repeated until the desire total heating time is reached.

Results

We see from **Fig. 4** and **Fig. 5** that the temperature rise in radial flow is less than for linear flow. This result is because of dilution of the EM energy rate caused by the expanding cross-sectional area for radial flow. The dilution would be even larger for spherical flow. At a given position counter-current flow always results in a smaller T than does co-current flow for radial flow. Evidently heat generated in the reservoir is returned to the well in such flow; the higher the flow rate, the more heat is produced. This effect is evident also in that the T increase in co-current flow penetrates deeper into the formation. The effect of a large EM adsorption is to cause a large T near the original wellbore. The effect of increasing adsorptivity is discussed further below. There is in all cases a trade-off between a large penetration distance and a large T at the wellbore.

Temperatures in the near wellbore zone as well as the advance of the heated front into the formation are also affected by the production rate for counter-current flow. As the amount of oil produced increases, more of the heat generated by EM is extracted from the formation. This decreases the temperature rise in the formation, and moreover the effectiveness of EM heating because the EM energy is constantly reheating the near wellbore area instead of propagating the heated front into the reservoir. (See **Fig. 6**)

Conduction has an important effect on the solutions. **Fig. 7** shows the effect of conduction in the temperature distribution for Cartesian counter-current flow. For radial flow **Fig. 8** shows a larger effect when conduction is considered increasing the temperature only about 80K compared to a 290K increment when this effect is neglected for the 140MHz frequency value of the adsorption coefficient. A constant rate of 30 BOPD was assumed, and the adsorption coefficient (α) for a 140 MHz frequency (0.01 m^{-1}) and a 915 MHz frequency (0.1 m^{-1}) used to evaluate the effect of conduction at different frequencies. The temperature near the source increases about 170K when conduction is neglected, but the rise is only about 80K when it is considered for linear flow for the low value of the adsorption coefficient. Using the higher adsorption coefficient value, although a higher temperature near the EM source is achieved when neglecting conduction, it declines sharply within 10 m from that while it goes further into the reservoir when there is conduction.

To show the effect of the adsorption coefficient on steady-state solutions we used a value of 4 BOPD for an 11°API crude. **Fig. 9** shows a PI for counter-current linear flow of about 2.5 times for a power input of 20 kW. The PI increases as the power in the source increases. For an input power of 150 kW, the PI improvement was about 12. For all the values used for the input power, the peak in the PI occurred within the range of $\alpha = 10^{-3}$ and 10^{-1} m^{-1}, which indicates the existence of an optimum adsorption coefficient. When the α increases beyond this point, a considerable reduction in the PI occurs. A large α represents resistive heating; evidently EM heating can outperform resistive heating in these solutions. For linear co-current flow the PI was even greater for the same values of input power than in counter-current flow. **Fig. 10** shows a maximum PI of about 40 times for a power of 150 kW. This is more than three times the value obtained for the counter-current flow case. However, when α increases beyond 10^{-1} m^{-1}, production declines back to the initial production rate.

For radial counter-current flow the maximum PI increase was about 4.6 times the cold production for an input power of 150 kW. This is approximately one third of the improvement obtained for linear flow, which shows that the effect of conduction is more important in radial than it is in linear flow, reducing the rise in temperature in the near wellbore zone, and therefore the PI. **Fig. 11** shows the PI for radial counter-current flow for different values of input power. Unlike linear flow, the maximum production occurred within the range of $\alpha = 10^{-2}$ and 10 m^{-1}.

Transient solutions for radial counter-current flow show the temperature increases with radiation time, and the heated zone extends further into the reservoir to approach steady-state solutions. Consequently, the PI increases as time progresses. However, the time to reach steady state changes significantly from one to ten years depending on whether the well is producing at a constant rate or at a constant pressure. When the pressure drop is fixed and the rate increases progressively, more of the heat is withdrawn from the reservoir and a steady state temperature takes longer to be reached compared to the constant rate case. **Fig. 12** shows how the temperature profile varies with time for radial counter-current flow. The time to achieve steady state is less than a year for a relatively small production rate. It takes longer to achieve steady state for co-current flow even producing at the same rate (See **Fig. 13**). This is because the EM energy must travel a longer distance to cause the rise in temperature necessary to move the oil near the producing well without the aid of a transporting fluid. However, the PI for co-current flow is higher than for counter-current flow for a constant pressure drop when they are compared at the same time because in co-current flow most of the EM energy remains in the reservoir while producing as opposed to counter-current flow.

Discussion

This study presents a single-phase model to calculate the temperature distribution and the productivity improvement for heavy-oil recovery when using EM heating. Results showed the existence of a maximum PI for what we have called an optimum adsorption coefficient, therefore an accurate determination of this parameter for the successful application of this technique is important. When the value used for the adsorption coefficient is too small (by using the wrong frequency), not enough heat is generated within the formation. Since fluid flow is taking place concurrently, this heat is extracted from the formation before it raises the formation temperature enough to cause a significant reduction in the oil viscosity to improve oil production. On the other hand, a very large adsorption coefficient represents that the EM energy is absorbed almost instantaneously into the formation so the heated zone does not extend into the reservoir.

Resistive heating is a special case of EM heating where low AC frequency is commonly used. Although electric current from low frequency tools penetrates deeper into the reservoir than high frequency, the rise in temperature of the heated zone is not as high as it can be when using high frequency EM heating. During resistive heating, energy is immediately absorbed into the formation so the temperature rise is small compared to EM heating. As a consequence, it is possible to get better oil production rates when EM heating is used.

Another important insight provided from this study is that EM heating for co-current flow gives a better productivity improvement than counter-current flow.

Conclusions

We developed a single-phase model to calculate the temperature distribution, and the productivity improvement obtained when an EM heating source is placed in a well. Results lead to the following conclusions:

1. Using the steady-state temperature distributions, we calculated the maximum PI improvement obtained from EM heating. Linear flow counter-current solutions showed an improvement of up to 12, while with co-current flow up to 36, for the same value of power used. For radial flow the PI was about one third of the value obtained for linear flow. Although these results were obtained for the specific reservoir and oil properties used, they confirm EM heating as a promising technique for heavy-oil recovery.
2. The PI improvement showed a maximum value at a finite adsorption coefficient. This finding suggests that EM heating can be more efficient than resistive heating.
3. When thermal conduction is significant, a smaller temperature rise in the near wellbore zone occurs compared to when conduction is neglected. This effect is more important for radial than for linear flow. Therefore, heat transfer by conduction should not be neglected when calculating the temperature distribution for EM heating.
4. Transient solutions showed that when the production rate is fixed, steady state is achieved earlier compared to when the rate is allowed to increase by fixing the pressure drop.
5. Co-current flow yields better oil production rates than counter-current flow. Transient solutions showed that as the heated front advances into the formation more energy is allocated within the reservoir causing the oil rate to increase more rapidly than for counter-current production. However, after two years of production the change in temperature is reduced which minimizes the change in the oil rate.

Acknowledgements

Larry W. Lake holds the W. A. (Monty) Moncrief Centennial Chair at The University of Texas.

Nomenclature

A = Cross sectional area (L^2)
c_t = total reservoir compressibility (L^2/F)
D = empirical constant for viscosity correlation (M/Lt)
F = empirical constant for viscosity correlation (T)
h = thickness (L)
J = productivity index (L^4t/M)
k = permeability (L^2)
k_T = thermal conductivity (ML/t^3T)
L = length (L)
M = volumetric heat capacity (M/Lt^2T)
P = pressure (M/Lt^2)
P_0 = power input (ML^2/t^3)
q_o = oil production rate (L^3/t)
q^r = EM heat flux (M/t^3)
q_0^r = EM heat flux at inner boundary (M/t^3)
r = radius (L)
r_w = wellbore radius (L)
T = temperature (T)
t = time (t)
u = fluid velocity (L/t)

Greek alphabets

α = adsorption coefficient (1/L)
ϕ = porosity, fraction
μ = fluid viscosity (M/Lt)

Subscripts

c = cold
h = heated
o = oil
T = total

References

Abernethy, E.R. 1976. Production Increase of Heavy Oil by Electromagnetic Heating. *J. Cdn. Pet. Tech* **15** (3): 91-97.

Araque, A. and Lake, L.W. 2002. Aspectos Relevantes Sobre Flujo de Fluidos Bajo Calentamiento Electromagnético. PDVSA-Intevep, INT 9388.

Baylor, B.A. and Wattenbarger, R.A. 1990. Improved Calculation of Oil Production Response to Electrical Resistance Heating (ERH). Paper SPE 20482 presented at the 85th SPE Annual Technical Conference and Exhibition, New Orleans, Louisiana, 23-26 September.

Bridges, J.E, Sresty, G.C, Spencer, H.L. and Wattenbarger, R. A. 1985. Electromagnetic Stimulation of Heavy-Oil Wells. Paper presented at the Third International Conference on Heavy Crude and Tar Sands. Long Beach, California.

Bird, R.B., Steward, W.E. and Lightfoot, E.N. 2002. *Transport Phenomena*, 506-507. New York City: John Wiley & Sons, Inc.

Callarotti, R.C. 2007. Electromagnetic Heating of Oil. *Emerging and Peripheral Technologies*, Chap. 12, Petroleum Engineering Handbook, Vol 6.

Chakma, A. and Jha, K.N. 1992. Heavy Oil Recovery From Thin Pay Zones by Electromagnetic Heating. Paper SPE 24817 presented at the 87th SPE Annual Technical Conference and Exhibition, Washington, DC, 4-7 October.

COMSOL AB. 2007. *COMSOL Multiphysics Modeling Guide*, 237-290.

Fanchi, J.R. 1990. Feasibility of Reservoir Heating by Electromagnetic Irradiation. Paper SPE 20483 presented at the 65th SPE Annual Technical Conference and Exhibition, New Orleans, Louisiana, 23-26 September.

Haagensen, A.D. 1965. Oil Well Microwave Tools. US Patent No. 3,170,119.

Hiebert, A.D., Vermeulen, F.E., Chute, F.S. and Capjack, C.E. 1986. Numerical Simulation Results for the Electrical Heating of Atabasca Oil-Sand Formations. *SPERE* **1** (1): 76-84.

Islam, M.R., Wadadar, S.S. and Bansal, A. 1991. Enhanced Oil Recovery of Ugnu Tar Sands of Alaska using Electromagnetic Heating With Horizontal Wells. Paper SPE 22177 presented at the International Arctic Technology Conference, Anchorage, Alaska, 29-31 May.

Kasevich, R.S., Price, S.L., Faust, D.L. and Fontaine, M.F. 1994. Pilot Testing of a Radio Frequency Heating System for Enhanced Oil Recovery From Diatomaceous Earth. Paper SPE 20483 presented at the 69th SPE Annual Technical Conference and Exhibition, New Orleans, Louisiana, 25-28 September.

Kim, E.S. 1987. Reservoir Simulation of in situ Electromagnetic Heating of Heavy Oils. PhD dissertation, Texas A & M U., College Station, Texas.

McGee B.C.W. and Vermeulen, F.E. 1996. Electrical Heating with Horizontal Wells, The Heat Transfer Problem. Paper SPE 37117 presented at the 1996 SPE International Conference on Horizontal Well Technology, Calgary, Canada, 18-20 November.

McPherson, R.G., Chute, F.S. and Vermeulen, F.E. 1985. Recovery of Atabasca Bitumen with the Electromagnetic Flood Process. *J. Cdn. Pet. Tech* **24** (1): 44-51.

Ovalles, C., Fonseca, A., Lara, A., et al. 2002. Opportunities of Downhole Dielectric Heating in Venezuela: Three Case Studies Involving Medium, Heavy, and Extra-Heavy Crude Oil Reservoirs. Paper SPE 78980 presented at the SPE International Thermal Operations and Heavy Oil Symposium, Calgary, Alberta, Canada, 4-7 November.

Sahni, A., Kumar, M., Knapp, R.B. and Livermore, L. 2000. Electromagnetic Heating Methods for Heavy Oil Reservoirs. Paper SPE 62550 presented at the 2000 SPE/AAPG Western Regional Meeting, Long Beach, California, 19-23 June.

Sierra, R., Tripathy, B., Bridges, J.E. and Farouq Ali, S.M. 2001. Promising Progress in Field Application of Reservoir Electrical Heating Methods. Paper SPE 69709 presented at the SPE International Thermal Operations and Heavy Oil Symposium, Margarita, Venezuela, 12-14 March.

Wattenbarger, R.A. and McDougal, F.W. 1988. Oil Production Response to in situ Electrical Resistance Heating. *J. Cdn. Pet. Tech* **27** (6): 45-50.

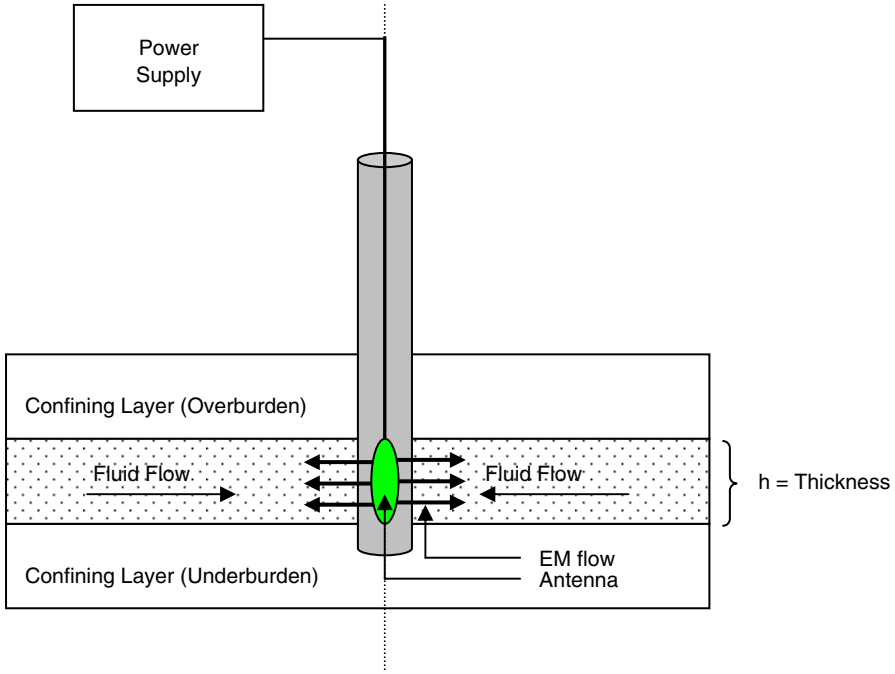

Fig. 1—Schematic view of EM heating for counter-current flow.

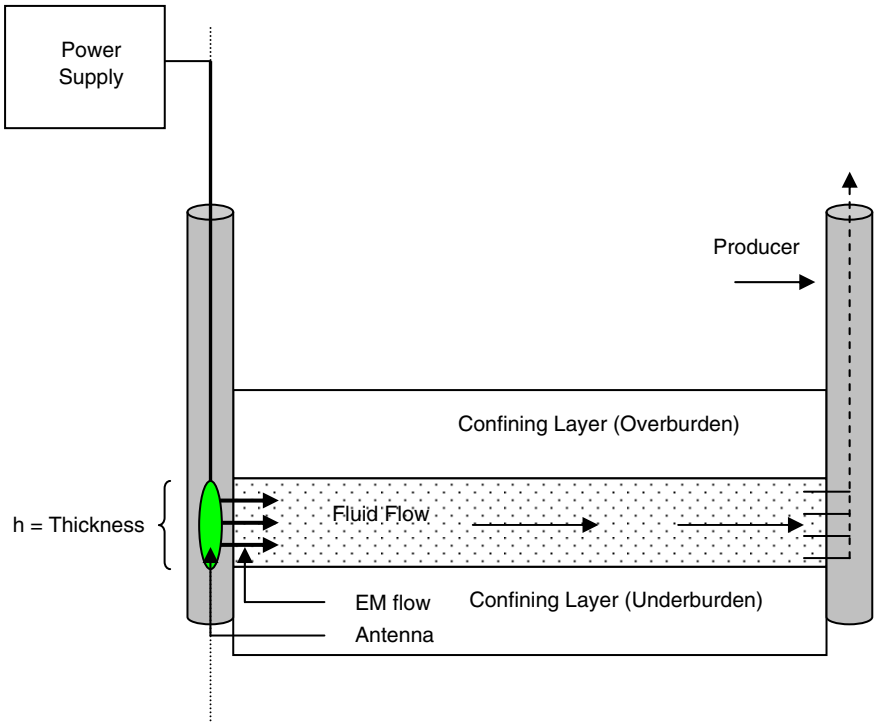

Fig. 2—Schematic view of EM heating for co-current flow.

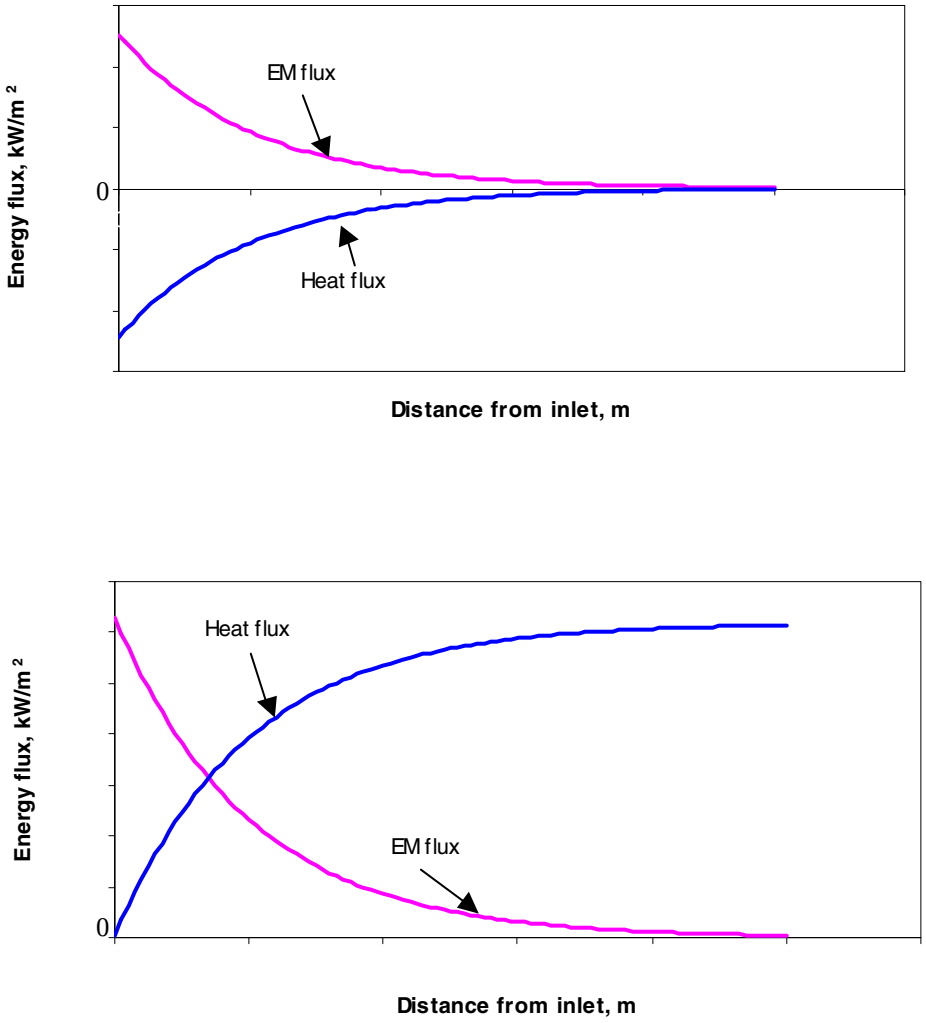

Fig. 3—Schematic comparison of energy fluxes for counter-current flow (top), and co-current flow (bottom).

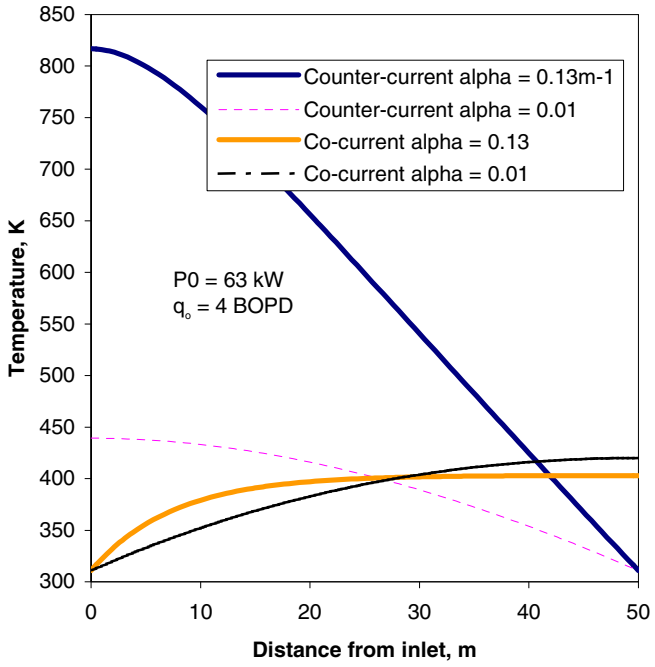

Fig. 4—Steady-state temperature profile for counter-current and co-current Cartesian flow for different values of the EM adsorption coefficient, α.

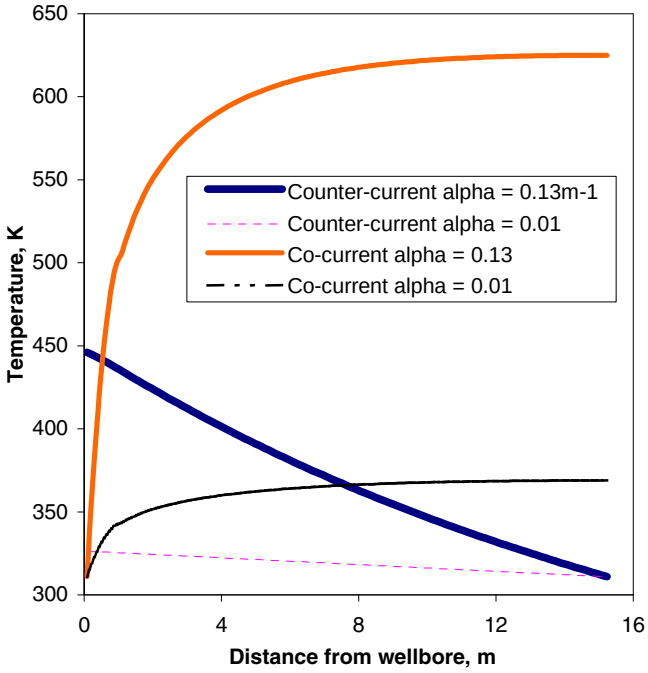

Fig. 5—Steady-state temperature profile for counter-current and co-current radial flow for different values of the EM adsorption coefficient, α.

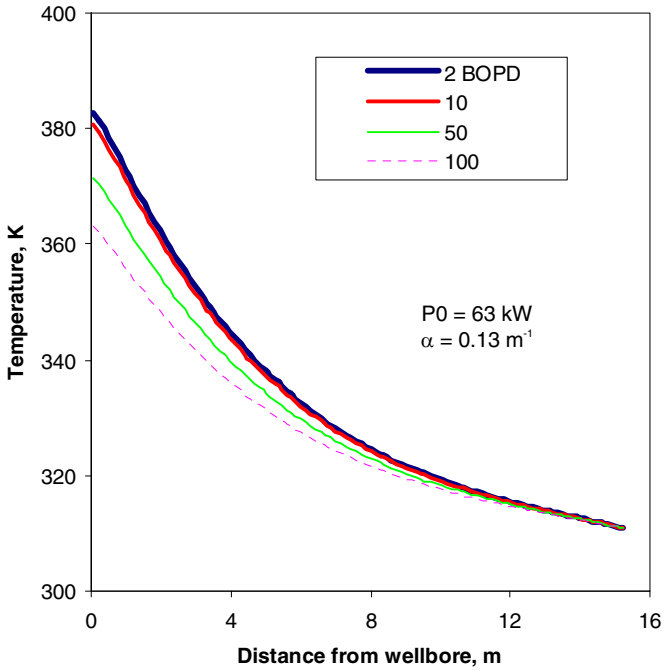

Fig. 6—Effect of the oil flow rate (q_o), on the temperature profile for counter-current radial flow after 30 days.

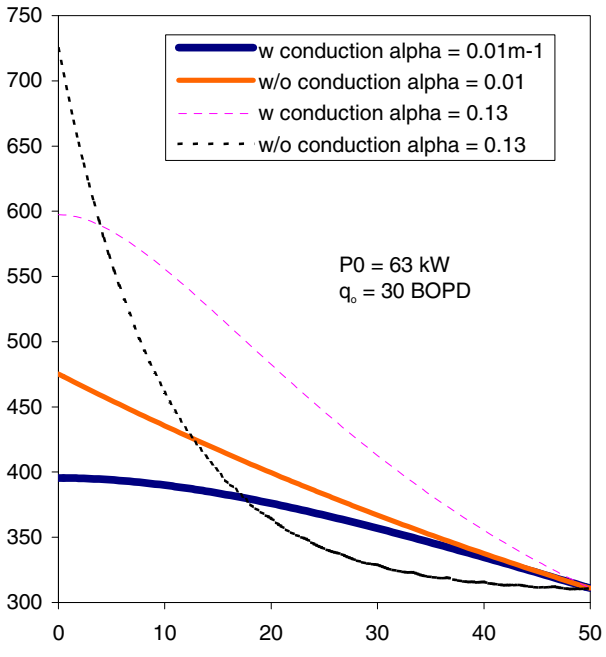

Fig. 7—Effect of conduction heat transfer on the ar steady state temperature profile for Cartesian counter-current flow for different values of the adsorption coefficient, α.

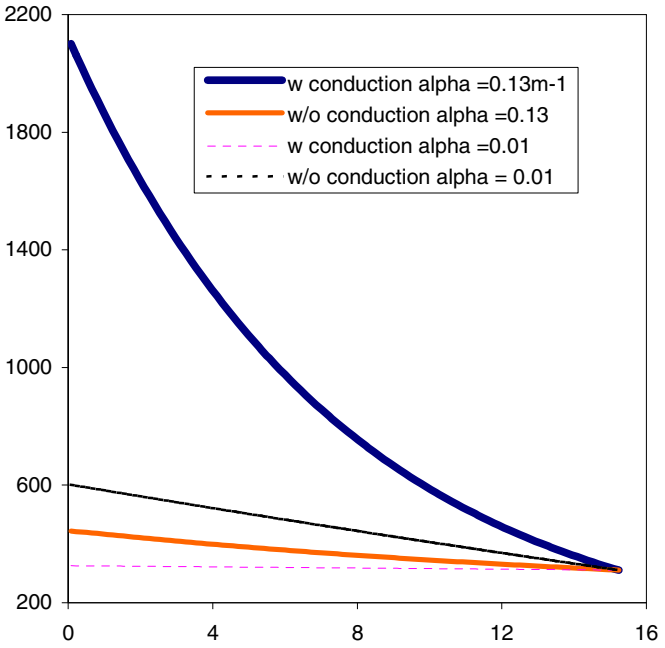

Fig. 8—Effect of conduction heat transfer on the radial steady state temperature profile for radial counter-current flow for different values of the adsorption coefficient, α.

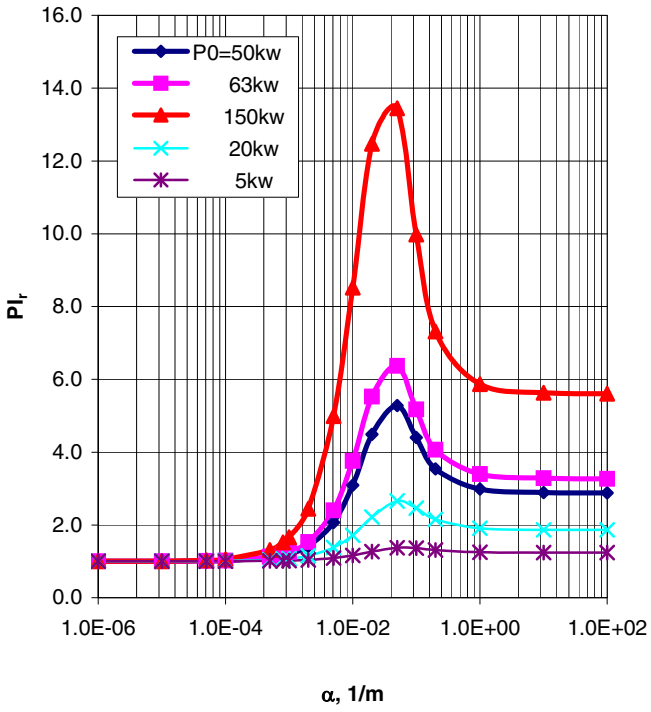

Fig. 9—Relative productivity index (PI) for Cartesian counter-current flow as a function of the adsorption coefficient (α), for different input power values.

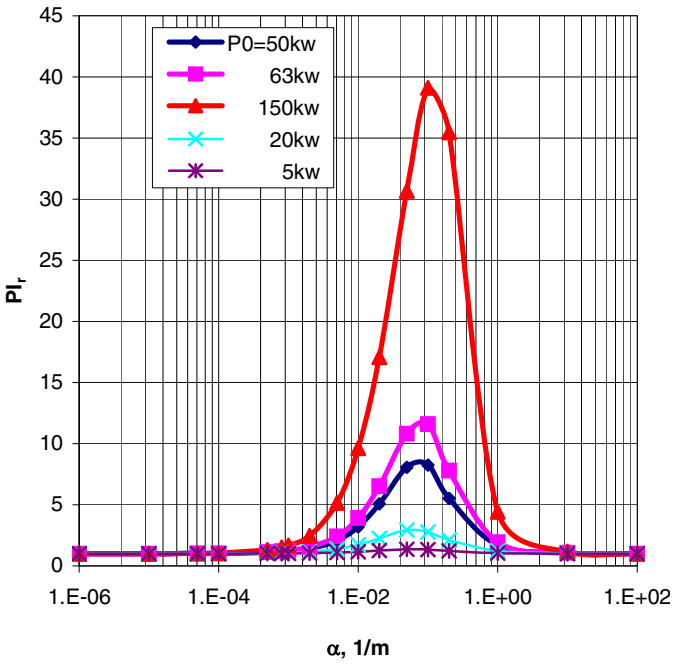

Fig. 10—Relative productivity index (PI) for Cartesian co-current flow as a function of the adsorption coefficient (α), for different input power values.

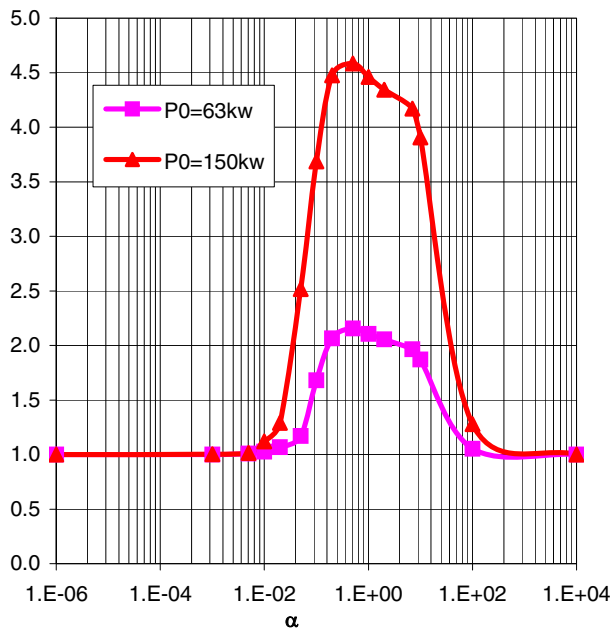

Fig. 11—Relative productivity index (PI) for radial co-current flow as a function of the adsorption coefficient (α), for different input power values.

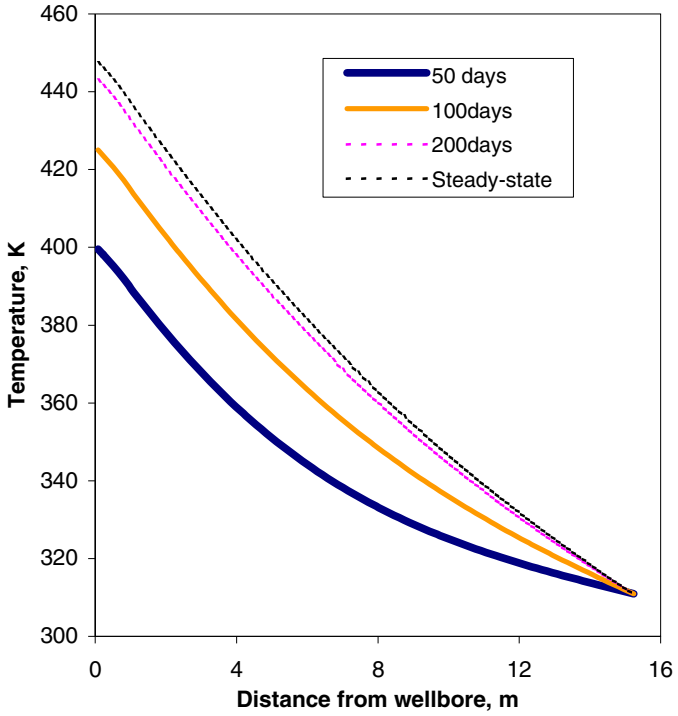

Fig. 12—Temperature profile variation with time for radial counter-current flow at a constant oil production rate (q_o).

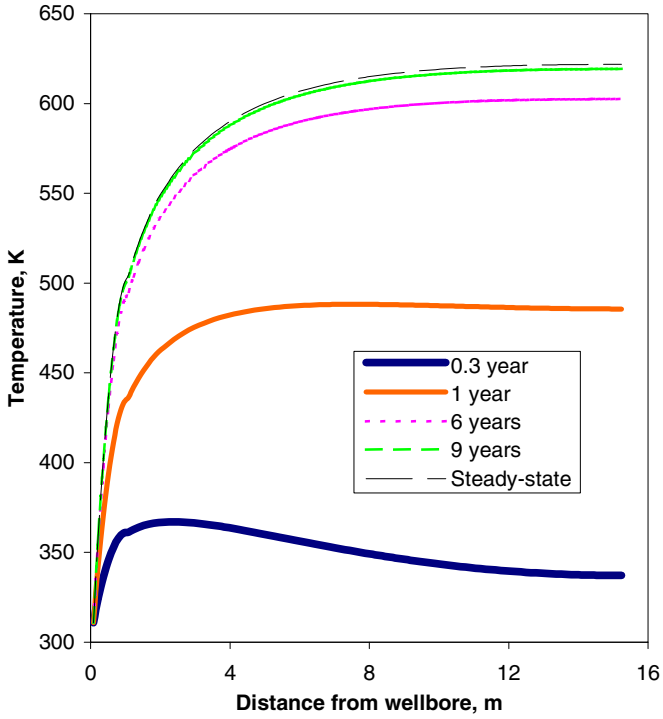

Fig. 13—Temperature profile variation with time for radial co-current flow at a constant oil production rate (q_o).

Appendix A

A detailed derivation of the analytical solutions for the temperature distribution for counter and co-current linear and radial flow is presented. These solutions were used to validate the results obtained from COMSOL Multiphysics.

a) Steady-State Temperature. Linear Flow

Considering steady state (SS), Eq. 1 for Cartesian flow reduces to:

$$-M_o u_o \frac{dT}{dx} + \frac{dq^c}{dx} + \frac{dq^r}{dx} = 0 \tag{A-1}$$

Let's do a variable change to simplify the solution, taking $T^* = T - T_0$ the one-dimensional energy flux (e) is:

$$e = -M_o u_o T^* - k_T \frac{dT^*}{dx} \tag{A-2}$$

Substitution of Eq. A-2 into Eq. A-1 yields:

$$\frac{de}{dx} + \frac{dq^r}{dx} = 0 \tag{A-3}$$

The boundary conditions represented by Eq. A-4 and Eq. A-5 describe the assumption of constant temperature at the outer boundary, and the symmetry of flow at the inner boundary respectively.

$$T^* = 0 \quad @\ x = L \tag{A-4}$$

$$\left(\frac{dT^*}{dx} \right)\Big|_{x=0} = 0 \tag{A-5}$$

The term that represents the EM source in Eq. A-1, can be expressed in a similar form to Abernethy's power attenuation tern as:

$$q^r = q_0^r e^{-\alpha x} \tag{A-6}$$

Counter-current Flow

The velocity u_o is positive in the –x direction. Integration of Eq. A-3 reduces the order of the PDE to be solved. Substitution of Eq. A.6 into the result of that integration, and then into Eq. A-2 yields:

$$\frac{q_0^r}{k_T} e^{-\alpha x} - \frac{C_0}{k_T} = \frac{M_o u_o}{k_T} T^* + \frac{dT^*}{dx} \tag{A-7}$$

Solution of Eq. A-7 gives the counter-current steady state temperature distribution as:

$$T^* = \frac{q_0^r}{u_o M_o - \alpha k_T}\left(e^{-\alpha x} - e^{-\alpha L}\right) + \frac{\alpha q_0^r k_T}{\left(u_o M_o - \alpha k_T\right) u_o M_o}\left(e^{\frac{-M_o u_o}{k_T}L} - e^{\frac{-M_o u_o}{k_T}x}\right) \tag{A-8}$$

then, back to the original variable T,

$$T = T_0 + \frac{q_0^r}{u_o M_o - \alpha k_T}\left(e^{-\alpha x} - e^{-\alpha L}\right) + \frac{\alpha q_0^r k_T}{\left(u_o M_o - \alpha k_T\right) u_o M_o}\left(e^{\frac{-M_o u_o}{k_T}L} - e^{\frac{-M_o u_o}{k_T}x}\right) \tag{A-9}$$

Co-current Flow

Now the velocity u_o is positive in the plus x direction so that, the PDE to be solved has the form:

$$\frac{dT^*}{dx} - \frac{M_o u_o}{k_T} T^* = \frac{q_0^r}{k_T} e^{-\alpha x} - \frac{C_0}{k_T} \tag{A-10}$$

with BC's

$$T^* = 0 \quad @\ x = 0 \tag{A-11}$$

$$\left(\frac{dT^*}{dx}\right)\Bigg|_{x=L} = 0\,. \tag{A-12}$$

Then, the co-current steady state temperature distribution is given by:

$$T^* = \frac{q_0^r}{u_o M_o + \alpha k_T}\left(1 - e^{-\alpha x}\right) + \frac{\alpha q_0^r k_T}{\left(u_o M_o - \alpha k_T\right) u_o M_o} e^{-\alpha L}\left(e^{\frac{-M_o u_o}{k_T}L} - e^{\frac{M_o u_o}{k_T}(x-L)}\right) \tag{A-13}$$

so that the original variable T is given by,

$$T = T_0 + \frac{q_0^r}{u_o M_o + \alpha k_T}\left(1 - e^{-\alpha x}\right) + \frac{\alpha q_0^r k_T}{\left(u_o M_o - \alpha k_T\right) u_o M_o} e^{-\alpha L}\left(e^{\frac{-M_o u_o}{k_T}L} - e^{\frac{M_o u_o}{k_T}(x-L)}\right) \tag{A-14}$$

b) Steady-State Temperature. Radial Flow

In radial coordinates the EM balance is:

$$\frac{1}{r}\frac{d(rq^r)}{dr} = -\alpha P(r) \tag{A-15}$$

with BC

$$\left(rq^r\right)_{r \to r_w} = P_0 \tag{A-16}$$

which solution is given by

$$P(r) = \frac{P_0}{r} e^{-\alpha(r - r_w)} \tag{A-17}$$

The energy flux (e) for radial flow can be defined as

$$e = -2\pi hM_o u_o T^* - 2\pi hk_T \frac{dT^*}{dr} \qquad \text{(A-18)}$$

where $T^* = T - T_0$. For radial flow Eq. A-3 can be written as:

$$\frac{d(re)}{dr} + \frac{d(rq^r)}{dr} = 0 \qquad \text{(A-19)}$$

Solution of Eq. A-19 has the following form

$$re = C_0 - P_0 e^{-\alpha(r-r_w)} \qquad \text{(A-20)}$$

Plugging Eq. A-18 into Eq. A-20 with the velocity u_o is positive in the –r direction, we get:

$$r\frac{dT^*}{dr} + \frac{M_o q_o}{2\pi hk_T} T^* = \frac{P_0}{2\pi hk_T} e^{-\alpha(r-r_w)} - \frac{C_0}{2\pi hk_T} \qquad \text{(A-21)}$$

Equation (A-21) has the following solution:

$$T^* = r^{-\frac{M_o q_o}{2\pi hk_T}} \left[\frac{P_0 e^{\alpha r_w}}{2\pi hk_T} \left[-r^{\frac{M_o q_o}{2\pi hk_T}} (\alpha r)^{-\frac{M_o q_o}{2\pi hk_T}} \Gamma\left(\frac{M_o q_o}{2\pi hk_T}, \alpha r \right) \right] - \frac{C_0}{M_o q_o} r^{\frac{M_o q_o}{2\pi hk_T}} + C_1 \right] \qquad \text{(A-22)}$$

where $\Gamma(a, \alpha r)$ is the upper incomplete gamma function, with special values

$$\begin{cases} \Gamma(a,0) = \Gamma(a) \\ \Gamma(a,\infty) = 0 \end{cases}$$

Finally, the stationary temperature profile is given by:

$$T^* = \frac{P_0 e^{\alpha r_w}}{2\pi hk_T} \left[-(\alpha r)^{-\frac{M_o q_o}{2\pi hk_T}} \Gamma\left(\frac{M_o q_o}{2\pi hk_T}, \alpha r \right) \right] - \frac{C_0}{M_o q_o} + C_1 r^{-\frac{M_o q_o}{2\pi hk_T}} \qquad \text{(A-23)}$$

with BC's:

$$T^*\Big|_{r=r_e} = T_0 \qquad \text{(A-24)}$$

$$\left(r\frac{dT^*}{dr} \right)\Bigg|_{r=r_w} = 0 \ . \qquad \text{(A-25)}$$

Then, the steady state temperature will be given by

$$\begin{aligned} T^* = {} & \frac{P_0 e^{\alpha r_w}}{2\pi hk_T} \left[\left(\frac{r_e}{r} \right)^{\frac{M_o q_o}{2\pi hk_T}} (\alpha r_e)^{-\frac{M_o q_o}{2\pi hk_T}} \Gamma\left(\frac{M_o q_o}{2\pi hk_T}, \alpha r_e \right) - (\alpha r)^{-\frac{M_o q_o}{2\pi hk_T}} \Gamma\left(\frac{M_o q_o}{2\pi hk_T}, \alpha r \right) \right] \\ & + \frac{P_0}{M_o q_o} \left(\left(\frac{r_e}{r} \right)^{\frac{M_o q_o}{2\pi hk_T}} - 1 \right) + T_0 \left(\frac{r_e}{r} \right)^{\frac{M_o q_o}{2\pi hk_T}} + \left(1 - \left(\frac{r_e}{r} \right)^{\frac{M_o q_o}{2\pi hk_T}} \right) T^*\Big|_{r_w} \end{aligned} \qquad \text{(A-26)}$$

where $T^*\Big|_{r_w}$ is the temperature at the wellbore defined as

$$T^*\Big|_{r_w} = \frac{\begin{aligned} & \frac{P_0 e^{\alpha r_w}}{2\pi hk_T} \left[\left(\frac{r_e}{r_w} \right)^{\frac{M_o q_o}{2\pi hk_T}} (\alpha r_e)^{-\frac{M_o q_o}{2\pi hk_T}} \Gamma\left(\frac{M_o q_o}{2\pi hk_T}, \alpha r_e \right) - (\alpha r_w)^{-\frac{M_o q_o}{2\pi hk_T}} \Gamma\left(\frac{M_o q_o}{2\pi hk_T}, \alpha r_w \right) \right] \\ & + \frac{P_0}{M_o q_o} \left(\left(\frac{r_e}{r} \right)^{\frac{M_o q_o}{2\pi hk_T}} - 1 \right) + T_0 \left(\frac{r_e}{r_w} \right)^{\frac{M_o q_o}{2\pi hk_T}} \end{aligned}}{\left(\frac{r_e}{r_w} \right)^{\frac{M_o q_o}{2\pi hk_T}}} \qquad \text{(A-27)}$$

c) Transient Temperatures. No Conduction

For counter-current radial flow, neglecting conduction, and using the attenuation term developed by Abernethy, the energy balance reduces to

$$M_T \frac{\partial T}{\partial t} = \frac{M_o q_o}{2\pi h} \frac{1}{r} \frac{\partial T}{\partial r} + \frac{\alpha P_0 e^{-\alpha(r-r_w)}}{2\pi r h} \tag{A-28}$$

where the total volumetric heat capacity (M_T) is given by

$$M_T = \phi M_o + (1-\phi) M_r \tag{A.29}$$

To simplify Eq. A-28, we define the variable $\xi = r^2$, then $d\xi = 2rdr$. Substitution of this into A-15 gives:

$$M_T \frac{\partial T}{\partial t} = \frac{M_o q_o}{\pi h} \frac{\partial T}{\partial \xi} + \frac{\alpha P_0 e^{-\alpha(\xi^{1/2} - \xi_0^{1/2})}}{2\pi h \xi^{1/2}}. \tag{A-30}$$

In dimensionless form Eq. A-30 can be written as

$$\frac{\partial T_D}{\partial t_D} - \frac{\partial T_D}{\partial \xi_D} = \frac{\alpha_D}{2\xi_D^{1/2}} e^{-\alpha_D\left(\xi_D^{1/2} - \xi_{Dw}^{1/2}\right)} \tag{A-31}$$

with BC's

$$\begin{cases} T_D(\xi_D, 0) = 0 \\ T_D(1, t_D) = 0 \end{cases}$$

where:

$t_D = \dfrac{M_o q_o}{\pi h M_T \xi_e} t$, $\alpha_D = \alpha \xi_e^{1/2}$, $T_D = \dfrac{M_o u_o}{P_0}(T - T_o)$, and $\xi_D = \dfrac{\xi}{\xi_e}$.

Applying Laplace transforms, Eq. A-31 can be transformed into:

$$\frac{d\overline{T_D}}{d\xi_D} - s\overline{T} = \frac{\alpha_D}{2s\xi_D^{1/2}} e^{-\alpha_D\left(\xi_D^{1/2} - \xi_{Dw}^{1/2}\right)} \tag{A-32}$$

with BC

$L\{T_D(1, t_D)\} = \overline{T_D}(1, s) = 0$.

Solution of Eq. A-32 using the given BC, gives:

$$T_D = \begin{cases} -e^{-\alpha_D\left[(t_D+\xi_D)^{1/2} - \xi_{Do}^{1/2}\right]} + e^{-\alpha_D\left[\xi_D^{1/2} - \xi_{Do}^{1/2}\right]} & \xi_D < 1 - t_D \\ e^{-\alpha_D\left[\xi_D^{1/2} - \xi_{Do}^{1/2}\right]} - e^{-\alpha_D\left[1 - \xi_{Do}^{1/2}\right]} & \xi_D > 1 - t_D \end{cases} \tag{A-33}$$

Similar procedure was used for the linear flow case, obtaining the solution

$$T_D = \begin{cases} -e^{-\alpha_D(t_D + x_D)} + e^{-\alpha_D x_D} & x_D < 1 - t_D \\ e^{-\alpha_D x_D} - e^{-\alpha_D} & x_D > 1 - t_D \end{cases} \tag{A-34}$$

where:

$t_D = \dfrac{M_o u_o}{M_T L} t$, $\alpha_D = \alpha L$, $T_D = \dfrac{M_o u_o}{P_0}(T - T_o)$, and $x_D = \dfrac{x}{L}$.

Appendix B. Productivity Improvement for Steady-State Solutions

The objective of this Appendix is to derive the equations used to calculate productivity improvement PI. The most important point here are that the PI equation applies to any one-dimensional flow geometry. Remember that the oil viscosity changes with position and time according to the solution to the energy balance, or

$$\mu_o = \mu_o(T) = \mu_o\big(T(t,x)\big) = \mu_o(t,x) \tag{B-1}$$

Starting with the conservation of oil in a medium for which the cross-sectional area changes with position, or $A = A(x)$

$$\frac{\partial(\phi\rho_o S_o)}{\partial t} + \frac{\partial(A\rho_o\mu_o)}{\partial x} = 0 \tag{B-2}$$

we assume that the porosity ϕ, oil density ρ_o , and oil saturation S_o are constant resulting in

$$\frac{d(Au_o)}{dx} = 0 \quad \text{or}$$

$$Au_o = q_o = q_o(t). \tag{B-3}$$

Equation B-3 says that the volumetric flow rate of oil q_o is a function of time only; it does not depend on position. These incompressibility assumptions are well suited for the types of flow normally encountered in heavy oil reservoirs. Now we introduce a gravity-free version of Darcy's Law into Eq. B-3

$$q_o = -\frac{Ak_o}{\mu_o}\frac{\partial P}{\partial x}.$$

Because of Eq. B-3 this equation can be integrated between the points o (outer) and i (inner) as

$$P_o - P_i = \Delta P = \frac{q_o}{k_o}\int_{x=x_o}^{x=x_i}\frac{\mu_o}{A}\,dx. \tag{B-4}$$

Equation B-4 has assumed that the oil phase permeability is independent of position; this could easily be accounted for if needed. Solving Eq. B-4 for the productivity index for the oil phase gives

$$J_o = \frac{q_o}{\Delta P}\left(\int_{x=x_o}^{x=x_i}\frac{\mu_o}{A}\,dx\right)^{-1}. \tag{B-5}$$

J_o is a function of time through Eq. B-1 even though time does not appear explicitly. This paper references the productivity indices to the cold oil value

$$J_{oc} = \frac{k_o}{\mu_{oc}}\left(\int_{x=x_o}^{x=x_i}\frac{dx}{A}\right)^{-1}$$

From this equation and Eq. B-5 the relative productivity index (*PI*), defined as the ratio of the production rate after EM heating to the cold production rate follows

$$PI = \frac{J_o}{J_{oc}} = \frac{\mu_{oc}\int_{x=x_o}^{x=x_i}\frac{dx}{A}}{\int_{x=x_o}^{x=x_i}\frac{\mu_o}{A}\,dx} \tag{B-6}$$

Equation B-6 applies to any 1D coordinate system. Specific cases are:

Linear (Cartesian): A = constant; $x_o = 0, x_i = L; PI = \dfrac{\mu_{oc}L}{\int_{x=0}^{x=L}\mu_o\,dx}$

Radial (cylindrical): $A = 2\pi r; x_o = r_w, x_i = r_e; PI = \dfrac{\mu_{oc}\ln\left(\frac{r_e}{r_w}\right)}{\int_{x=r_w}^{x=r_e}\frac{\mu_o}{r}\,dr}$

Spherical: $A = 4\pi r^2; x_o = r_w, x_i = r_e; PI = \dfrac{\mu_{oc}\left(\frac{1}{r_w}-\frac{1}{r_e}\right)}{\int_{x=r_w}^{x=r_e}\frac{\mu_o}{r^2}\,dr}$

Linear flow is common for laboratory evaluation of EM heating, while radial and spherically flow occur within a reservoir.

The integrals in the denominator in these definitions are handled numerically. The *PI* calculated from these formulas applies to both constant rate and constant ΔP flow; however, the viscosity-temperature relationship Eq. B-3 will depend strongly on these boundary conditions; hence, the calculated results will depend on the exact nature of the flow.